

RESEARCH

Open Access



Intravoxel incoherent motion magnetic resonance imaging and derived parameters in the assessment for polycystic ovary syndrome

Sercin Ozkok^{1*}, Mine Sorkun¹, Mahmut Bilal Dogan¹, Bulent Can², Meryem Hocaoglu³ and Ahmet Aslan¹

Abstract

Background: Polycystic ovary syndrome (PCOS) is the most common endocrinologic disorder in reproductive age. Diagnosis is based on clinical, laboratory, and ultrasonography findings. However, the application of ultrasound for the diagnosis of PCOS in overweight and sexually inactive patients may be limited. The purpose of this study was to display the imaging characteristics of intravoxel incoherent motion (IVIM) magnetic resonance imaging (MRI)-derived parameters as D_{true} (slow diffusion coefficient), D^* (perfusion-related diffusion), f (perfusion fraction), and apparent diffusion coefficient (ADC) in PCOS.

Results: A total of 43 women, 20 with PCOS (mean age, 24.09 ± 3.92 years) and 23 healthy control (mean age, 23 ± 1.67 years), were included. IVIM MRI-derived parameters of the ovarian stroma were measured by two observers. Mean D^* and f values were found to be higher in PCOS patients than in individuals in the control group ($p = 0.011$ and $p = 0.004$, respectively). The ADC value was found to be significantly lower in the patient group ($p = 0.003$). There was no statistically significant difference between two groups in D_{true} ($p = 0.742$). The interclass correlation analysis of two observers for both groups showed a good-to-excellent agreement. The ROC produced an AUC of 0.521, a sensitivity of 50%, a specificity of 57%, and a cut-off value of $1.48 \times 10^{-3} \text{ mm}^2/\text{s}$ for D_{true} ; an AUC of 0.769, a sensitivity of 55%, a specificity of 67%, and a cut-off value of $22.25 \times 10^{-3} \text{ mm}^2/\text{s}$ for D^* ; an AUC of 0.734, a sensitivity of 55%, a specificity of 62%, and a cut-off value of 20.87% for f ; an AUC of 0.893, a sensitivity of 90%, a specificity of 33%, and a cut-off value of $1.37 \times 10^{-3} \text{ mm}^2/\text{s}$ for ADC.

Conclusions: IVIM MRI would be an alternative imaging tool in the diagnosis of PCOS with a good-to-excellent agreement and with acceptable sensitivity and specificity.

Keywords: Polycystic ovary syndrome (PCOS), Intravoxel incoherent motion (IVIM), Magnetic resonance imaging (MRI), Diffusion, Perfusion

Background

Polycystic ovary syndrome (PCOS) is one of the most commonly seen endocrinologic disorders, with a prevalence of 6%–15% in reproductive age [1]. Although the

etiology of PCOS is not clarified, it is accepted as a multifactorial with several genetic, metabolic, and endocrine disorders [1]. The defect in secretion or action of the follicle-stimulating hormone (FSH) pathway is suggested to be the reason for impaired dominant follicle selection (1). Furthermore, hypothalamic-pituitary-gonadotropin imbalance causing more remarkable luteinizing hormone (LH) pulse amplitude and frequency lead to an altered LH / FSH ratio that results in follicular arrest [1]. PCOS is suggested to be associated with infertility, psychiatric

*Correspondence: sercinbas2005@gmail.com

¹ Department of Radiology, Goztepe Training and Research Hospital, Istanbul Medeniyet University, Istanbul, Turkey
Full list of author information is available at the end of the article

disorders, and metabolic diseases [2]. Thus, an accurate and certain diagnosis is essential.

PCOS has been defined as a condition of ovulatory disorder, hyperandrogenism, and polycystic appearance of ovaries on ultrasound in a consensus of the Rotterdam ESHRE/ASRM, 2003 [3]. For the diagnosis, 2 of 3 criteria are required with the elimination of other etiologies. Among these three criteria, ultrasonographic evaluation (12 or more follicles with 2–9 mm in diameter per ovary) and/or increase in ovarian volume (larger than 10 ml) is the most challenging component of the diagnosis [4]. Recommendation of ultrasonographic assessment of ovaries based on transvaginal approach [5, 6]. However, the transvaginal approach is contraindicated in virgin patients [5, 6]. And also, it has limited visualization of the ovaries because of the abdominal fat in overweighted patients [5]. Magnetic resonance imaging (MRI) demonstrated that ovarian morphology would be evaluated accurately and offered to be an alternative technique to ultrasound in overweighted and virgin patients [6–9]. In a study by Yoo et al., MRI is suggested to provide an increased spatial resolution of ovarian morphology with a higher follicle number than that revealed by transabdominal ultrasound [8]. However, functional MRI has not been applied yet. A noninvasive imaging technique not only for characterizing ovarian morphology but also for providing physiological information without using contrast agents is needed for diagnosis or monitoring the response to therapy.

Intravoxel incoherent motion (IVIM) MRI is a noninvasive modality that evaluates the tissue diffusion and microcapillary perfusion in separate calculations by a biexponential equation as distinct from diffusion-weighted imaging (DWI), which uses a monoexponential equation [9, 10]. In IVIM MRI, three additional parameters as true or slow diffusion coefficient, perfusion-related (pseudo or rapid) diffusion, and perfusion fraction (f) can be measured [9, 11–13]. It has been widely applied in liver pathologies, including hepatosteatosis, liver fibrosis, or in various malignancies such as ovarian, cervical, and breast carcinomas in recent years [14, 15]. As far as we know, IVIM MRI in the assessment of PCOS has not been performed yet. This study aimed to assess IVIM MRI-derived parameters in PCOS and to evaluate the IVIM MRI as a new diagnostic approach.

Methods

Subjects

Ethical approval of this prospective study was obtained from the Ethical Committee of the university hospital, and written informed consent was obtained.

A total of twenty patients who were diagnosed with PCOS according to the revised consensus on diagnostic

criteria [3, 4] by a ten years experienced gynecologist and endocrinologist and twenty-three healthy volunteers were included in this study between January 2019 and October 2020. The diagnosis of PCOS was performed according to the presence two criteria of three of the following: (1) ovarian dysfunction (oligo- or anovulation), (2) clinical and/or biochemical signs of hyperandrogenism, and (3) polycystic ovaries (presence of 12 or more follicles in each ovary measuring 2–9 mm) [3, 4].

The inclusion criteria were patients with 17 and 38 years of age. The exclusion criteria were the individuals with any endocrine (diabetes mellitus, hypothyroidism, hyperthyroidism, hyperprolactinemia, adrenal enzyme abnormality, etc.), systemic, and neoplastic disorders were excluded. The patients had ovarian cyst (larger than 3 cm) on transabdominal ultrasound. The patients who had claustrophobia and metallic implants /implantable devices contraindicated to MRI were also excluded.

Demographic and clinical data, including luteinizing hormone (LH), follicle-stimulating hormone (FSH), dehydroepiandrosterone, and dehydroepiandrosterone sulfate (DHEA), free testosterone, free T4, thyroid-stimulating hormone (TSH), glucose, insulin resistance, LH / FSH ratio, were retrieved from the data system.

Transabdominal ultrasound and pelvic MRI were obtained within the first week following the menstruation for all individuals in the control and patient groups. All transabdominal ultrasound evaluations were performed with an Aplio 500 ultrasound system machine (Toshiba Medical Systems, Tokyo, Japan) and a 9 MHz frequency convex array transducer by ten years experienced radiologist.

IVIM MRI examination and analysis

All MRIs were performed on a 1.5 T magnet field scanner (450 W; General Electric Medical Systems, Waukesha, Wisconsin, USA) with a 32-channel phased-array abdominal coil without contrast agent administration. Pelvic images were obtained in the axial plane using a 15 to 20 s breath-hold T2 weighted image and IVIM MRI sequence. Imaging parameters of the T2 weighted images sequence were applied as follows; repetition time 3.1 ms; the echo time 1 ms; flip-angle 58°; bandwidth \pm 108 kHz; matrix 192 \times 228; FOV 380 mm; the number of excitations 1; slice thickness 5 mm; gap 1 mm. Ten (10) b values (0, 10, 20, 30, 50, 80, 100, 200, 400, 800 s/mm²) were applied during the IVIM MRI sequence. The other parameters were as follows; repetition time 4.2 ms; the echo time 1.4–11 ms; flip-angle 35°; bandwidth \pm 55 kHz; matrix 320 \times 198; FOV 345 mm; Number of excitations 1; slice thickness 5 mm; gap 1 mm. The average scan time was 5–10 min for T2 weighted image and 5–10 min for IVIM MRI sequence.

All the MRI examinations were assessed by two radiologists with at least 8 years of experience blinded to patient information. IVIM MRI images were automatically processed on the device, and IVIM MRI-derived parameters [D_{true} , D^* , f , and apparent diffusion coefficient (ADC) maps] were produced. All the measurements were performed on a workstation (Advantage Workstation, General Electric Medical Systems, Waukesha, Wisconsin, USA). During the evaluation, an axial T2 weighted image was used to differentiate ovarian stroma from follicles to evaluate the number of ovarian follicles and ovarian volume (Fig. 1). Copied two round regions of interest (ROI) with 2–3 mm² were placed manually within each ovarian stroma in the IVIM MRI sequence (Fig. 1). The mean D_{true} , D^* , f , and ADC values were calculated by averaging the four measurements (two ROIs for left and two ROIs for right ovaries) for both observers. The mean values of IVIM MRI-derived parameters were recorded as average measurements of both observers.

Diffusion-weighted and intravoxel incoherent motion magnetic resonance imaging

DWI is a single-shot echoplanar imaging sequence with a long time to echo value with a motion-probing gradient pulse used to reduce the signal intensity of moving water molecules [16].

$$S_b = S_0 \exp(-b \times \text{ADC})$$

The magnitude of the water diffusion was described by the ADC. S_0 is the baseline signal intensity ($b=0$) recorded before the image acquisition, and the S_b is a signal intensity at a prescribed b value. Therefore, the signal intensity of different tissue decreases at different rates defined by their baseline signal intensity, ADC, and the b values [16]. IVIM MRI sequence is established on a bi-compartment model, which was first presented by Le Bihan et al. [9, 11]. According to this model, the increased signal in DWI was originated from the motion of water molecules in different compartments such as extracellular, intracellular, and intravascular space or perfusion [17]. Differentiating the motion of water molecules in intravascular space from diffusion in the extravascular

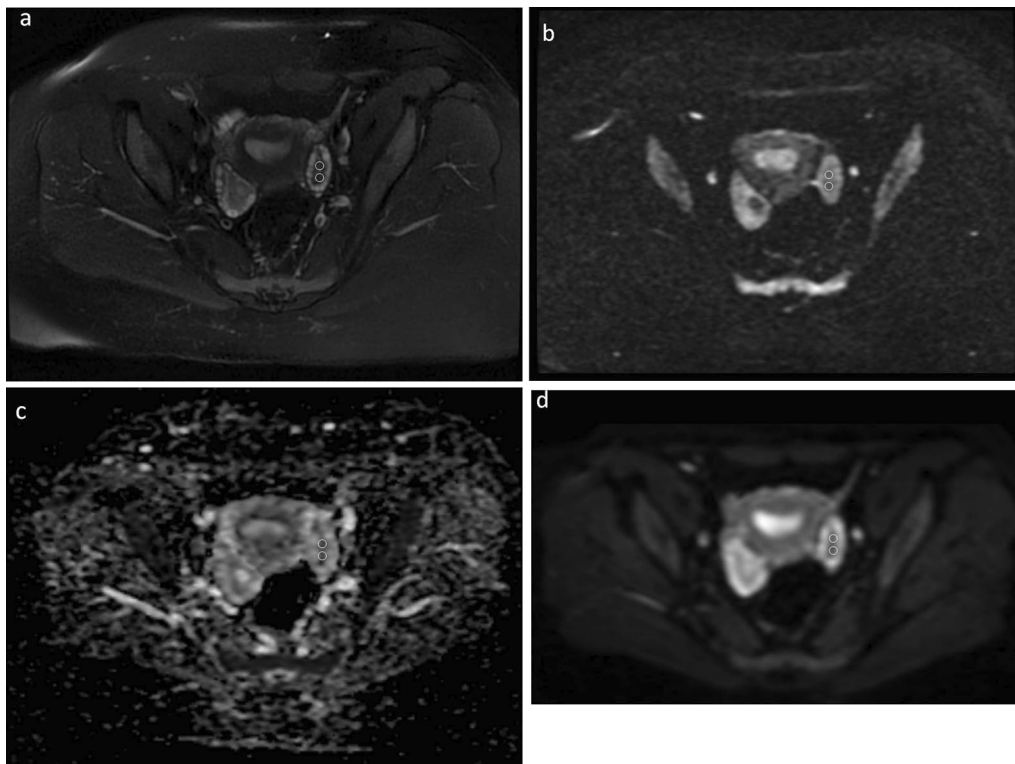


Fig. 1 a 20-year-old girl with polycystic ovary syndrome. **a–c** Axial T2 weighted images (fast imaging employing steady-state acquisition) sequence shows peripheral ovarian follicle and central stroma in the left ovary (**a**), two regions of interest (ROI) replaced in the ovarian stroma in a single-shot echo-planar diffusion-weighted image ($b = 800 \text{ s/mm}^2$) (**b**) and apparent diffusion coefficient (ADC) map (mm^2/s) (**c**), corresponding IVIM MRI sequence that used for derived parameters (**d**)

space is presented by the methodology of IVIM imaging [16]. S_b is the signal at a diffusion weighting with a specific b value, and S_0 is the signal intensity at baseline.

$$S_b = S_0 [(1 - f) \exp(-b \times D) + f \exp(-b \times D^*)]$$

D_{true} showed the apparent diffusivity of water and is affected by an increment of density in cellular structure [9, 18, 19]. D^* or pseudo-diffusion coefficient indicates intravascular blood flow velocity and perfusion fraction (f) shows blood volume, which reflects the capillary perfusion [19]. Thus, a lower D^* or f value indicates impaired capillary perfusion. In lower b -values, the intravoxel spin dephasing caused by the pseudorandom blood flow in the presence of diffusion gradient will promote more signal attenuation. During the following phase of the signal decay, the attenuation was mainly the result of the diffusion of water molecules because the blood signal would be suppressed to the higher diffusion gradients [20].

Statistical analysis

Normally distributed data are described as mean ± SD. Non-normally distributed data (free testosterone, free T4, and TSH) are presented as medians with interquartile range (interquartile range, IQR 25–75). Differences between two groups in IVIM MRI-derived parameters and laboratory findings were evaluated using an independent sample t test or Mann–Whitney U test. Laboratory findings were assessed with respect to IVIM-derived parameters using the Pearson or the Spearman correlation tests. All variables were analyzed for normality using Shapiro–Wilk tests, and a p -value of <0.05 was

considered a statistically significant difference. Statistical analyses were done using SPSS (SPSS 20, Chicago, Illinois, USA).

Interclass correlation coefficient (ICC) was assessed by a two-way mixed model. Both observers measured at 2 points of each ovary (4 ROI measurements for each patient). ICC (95% confidence interval [CI]) values of average measurements were obtained by the mean rating of 2 measurements for each observer. An ICC coefficient value higher than 0.8 indicates excellent agreement, 0.8–0.6 substantial agreement, 0.6–0.4 moderate agreement, and lower than 0.4 poor agreement [21]. Receiver operating characteristic (ROC) curve analyses were performed to determine the optimal cut-off values for each covariate (D , D^* , f , and ADC).

Results

A total of 43 females, 20 patients diagnosed with PCOS, and 23 healthy controls, were included in this study. There was no significant difference between the two groups in terms of the patient age: 24.09 ± 3.92 years (ranges: 18–31 years) vs. 23 ± 1.67 years (ranges: 21–26 years) ($p = 0.239$). Body mass index was higher in patient group (28.41 ± 7.14 vs. 22.14 ± 2.69 kg/m², $p = 0.001$). Demographic details with blood tests and ovarian morphologic characteristics are provided (Table 1). Blood tests showed PCOS patients had increased hormone levels compared to the control group. LH, DHEAS, free testosterone, TSH, insulin resistance and LH/FSH ratio were significantly higher in PCOS patients compared with the control group

Table 1 Demographic characteristics and laboratory parameters of polycystic ovary syndrome and control groups

	PCOS patients (n = 20)	Control group (n = 23)	p value	t value
Age (years)	24.09 ± 3.92	23 ± 1.67	0.239	1.193
Body mass index (kg/m ²)	28.41 ± 7.14	22.14 ± 2.69	0.001	3.645
LH (U/L)	5.93 ± 5.49	2.12 ± 0.76	0.008	2.931
FSH (U/L)	4.44 ± 2.14	4.56 ± 1.37	0.873	−0.163
DHEA (µg/dL)	430.59 ± 178.08	170.44 ± 58.91	<0.001	5.142
Free testosterone (nmol/lc)	2.29 (1.68–2.75)	1.017 (0.99–1.048)	<0.001	5.991
Free T4 (ng/dL)	0.96 (0.86–1.04)	0.98 (0.96–1.07)	0.613	−0.510
TSH (mIU/L)	1.76 (1.26–2.24)	1.29 (0.93–1.83)	0.048	2.047
Glucose (mmol/L)	89.09 ± 8.98	87.42 ± 8.77	0.605	0.524
Insulin resistance	1.67 ± 1.33	1.41 ± 1.05	0.018	2.445
LH/FSH ratio	1.22 ± 0.76	0.67 ± 0.46	0.013	2.614
Follicle count per ovary	20.84 ± 3.61	7.97 ± 2.82	<0.001	12.882
Ovarian volume (cm ³)	13.41 ± 3.15	8.05 ± 2.20	<0.001	6.368
D_{true} (× 10 ^{−3} mm ² /s)	1.51 ± 0.17	1.53 ± 0.25	0.742	0.331
D^* (× 10 ^{−3} mm ² /s)	27.88 ± 9.21	19.85 ± 10.52	0.011	−2.670
f (%)	23.15 ± 3.56	18.74 ± 5.61	0.004	−3.115
ADC (× 10 ^{−3} mm ² /s)	1.23 ± 0.26	1.42 ± 0.06	0.003	−3.292

($p=0.008$, $p<0.0001$, $p<0.0001$, $p=0.048$, $p=0.018$, $p=0.013$, respectively). There was no significant difference between the two groups in terms of the FSH, free T4, and glucose ($p=0.873$, $p=613$, and $p=605$, respectively). The mean follicle count and ovarian volume for single ovary were calculated as 20.84 ± 3.61 and $13.41 \pm 3.15 \text{ cm}^3$ in PCOS group and 7.97 ± 2.82 and $8.05 \pm 2.20 \text{ cm}^3$ in control group ($p<0.0001$, $p<0.0001$, respectively).

The mean D^* and f values in patient group (patient group: D^* ; $27.88 \pm 9.21 \times 10^{-3} \text{ mm}^2/\text{s}$, f ; $23.15 \pm 3.56\%$, control group: D^* ; $19.85 \pm 10.52 \times 10^{-3} \text{ mm}^2/\text{s}$, f ; $18.74 \pm 5.61\%$) were significantly higher ($p=0.011$ and $p=0.004$, respectively). The ADC value was significantly lower in patient group compared to the control group (ADC; $1.23 \pm 0.26 \times 10^{-3} \text{ mm}^2/\text{s}$, ADC; $1.42 \pm 0.06 \times 10^{-3} \text{ mm}^2/\text{s}$, $p=0.003$). There was no statistically significant difference in terms of D_{true} ($p=0.742$). IVIM MRI-derived parameters of bilateral ovaries in PCOS patients and controls are shown in Table 1. There was no statistically significant correlation between laboratory findings and IVIM MRI parameters in both groups (Table 2).

The interclass correlation analysis of two observers for both groups showed a good-to-excellent agreement for D_{true} , D^* , f , ADC values (Table 3). The interobserver agreement was for D_{true} : 0.844 (95% CI=0.612–0.938), for D^* : 0.891 (95% CI=0.725–0.957), for f : 0.711 (95% CI=0.257–0.887), for ADC: 0.820(95% CI=0.583–0.923) in PCOS group, respectively. And also the interobserver agreement was for D_{true} : 0.907 (95% CI=0.780–0.961), for D^* : 0.915 (95% CI=0.798–0.964), for f : 0.964 (95% CI=0.915–0.985), for ADC: 0.853 (95% CI= -0.139–0.967) in control group, respectively.

ROC curves were developed for each covariate (D , D^* , f , ADC) (Table 4). The ROC produced an AUC of 0.521 (ranges, 0.341–0.701), a sensitivity of 50%, a specificity of 57%, and a cut-off value of $1.48 \times 10^{-3} \text{ mm}^2/\text{s}$ for D_{true} ; an AUC of 0.769 (ranges, 0.625–0.914), a sensitivity of 55%, a specificity of 67%, and a cut-off value of $22.25 \times 10^{-3} \text{ mm}^2/\text{s}$ for D^* ; an AUC of 0.734 (ranges, 0.584–0.896), a sensitivity of 55%, a specificity of 62%, and a cut-off value of 20.87% for f ; an AUC of 0.893 (ranges, 0.774–1.013), a sensitivity of 90%, a specificity of 33%, and a cut-off value of $1.37 \times 10^{-3} \text{ mm}^2/\text{s}$ for ADC. Positive and negative predictive values are 53% and 58%

Table 2 Correlation of the values for IVIM MRI-derived parameters and laboratory findings of polycystic ovary syndrome group

	$D_{\text{true}} (D \text{ slow}) (\times 10^{-3} \text{ mm}^2/\text{s})$		$D^* (D_{\text{fast}}) (\times 10^{-3} \text{ mm}^2/\text{s})$		f (perfusion fraction) (%)		ADC (apparent diffusion coefficient) ($\times 10^{-3} \text{ mm}^2/\text{s}$)	
	p value	t value	p value	t value	p value	t value	p value	t value
LH (U/L)	0.188	-0.215	0.276	-0.142	0.448	-0.032	0.106	-0.301
FSH (U/L)	0.054	-0.380	0.103	-0.140	0.486	0.009	0.201	-0.204
DHEA ($\mu\text{g}/\text{dL}$)	0.368	-0.088	0.097	-0.337	0.352	-0.099	0.347	0.103
Free testosterone (nmol/lc)	0.165	-0.260	0.303	0.140	0.271	0.164	0.066	0.393
Free T4 (ng/dL)	0.285	0.128	0.296	-0.121	0.056	0.349	0.417	0.047
TSH (mIU/L)	0.447	-0.030	0.132	-0.249	0.072	-0.322	0.419	-0.046
Insulin (mmol/L)	0.476	0.015	0.436	-0.039	0.178	-0.231	0.117	-0.311
Insulin resistance	0.345	-0.088	0.178	-0.202	0.215	-0.173	0.266	0.263
LH/FSH ratio	0.338	0.094	0.278	-0.102	0.254	0.147	0.105	-0.278

Table 3 Mean values for IVIM MR-derived parameters and interobserver correlations in polycystic ovary syndrome and control groups

		Observer 1	Observer 2	ICC (95% CI)	p value
		PCOS patients ($n=20$)	$D_{\text{true}} (\times 10^{-3} \text{ mm}^2/\text{s})$	1.52 ± 0.18	1.49 ± 0.25
	$D^* (\times 10^{-3} \text{ mm}^2/\text{s})$	27.44 ± 11.88	28.38 ± 7.80	0.891 (0.725–0.957)	<0.0001
	f (%)	23.27 ± 4.45	23.02 ± 0.23	0.711 (0.257–0.887)	<0.0001
	ADC ($\times 10^{-3} \text{ mm}^2/\text{s}$)	1.27 ± 0.29	1.21 ± 0.25	0.820 (0.583–0.923)	<0.0001
Control patients ($n=23$)	$D_{\text{true}} (\times 10^{-3} \text{ mm}^2/\text{s})$	1.59 ± 0.36	1.53 ± 0.25	0.907 (0.780–0.961)	<0.0001
	$D^* (\times 10^{-3} \text{ mm}^2/\text{s})$	19.89 ± 11.21	19.81 ± 10.72	0.915 (0.798–0.964)	<0.0001
	f (%)	18.93 ± 5.94	18.54 ± 5.47	0.964 (0.915–0.985)	<0.0001
	ADC ($\times 10^{-3} \text{ mm}^2/\text{s}$)	1.47 ± 0.12	1.38 ± 0.36	0.853 (-0.139–0.967)	<0.0001

Table 4 Receiver operating characteristic analysis sensitivity–specificity analysis and determination of cut-off values for IVIM MRI-derived parameters

	D_{true} ($\times 10^{-3}$ mm ² /s)	D^* ($\times 10^{-3}$ mm ² /s)	f (%)	ADC ($\times 10^{-3}$ mm ² /s)
AUC (CI 95%)	0.521 (0.341–0.701)	0.769 (0.625–0.914)	0.734 (0.584–0.896)	0.893 (0.774–1.013)
Cut-off value	1.48	22.25	20,87	1.37
<i>p</i> value	0.817	0.003	0.009	<0.001
Sensitivity%	50	55	55	90
Specificity%	57	67	62	33
PPV%	53	61	58	62
NPV%	58	64	63	86
Standard error	0.092	0.074	0.077	0.061

for D_{true} , 61% and 64% for D^* , 58% and 63% for f , 62% and 86% for ADC, respectively.

Discussion

DW-MRI and ADC values are mentioned to have the potential of imaging biomarkers in Diffusion-Weighted Magnetic Resonance Imaging as a Cancer Biomarker: Consensus and Recommendations, 2009 [22]. Monoexponential DWI has been applied in various ovarian pathology, including ovarian tumors [23–25]. ADC measurement in gynecological disorders has been usually performed either in the evaluation of malignant tumors or in response to therapy. However, ADC assessment of PCOS is scarce [26, 27]. The study by Samancı et al. assessed ovarian stroma by monoexponential DWI and demonstrated significantly lower stromal ADC values in PCOS patients [27]. Similar findings were also revealed in a study by Deveer et al. [26]. In concordance with the results of the study by Deveer et al. and Samancı et al. [26, 27], we found decreased stromal ADC value in PCOS patients.

Decreased ADC values in malignant tumors are suggested to be related to a combination of increased cellularity and higher extracellular space tortuosity, all contributing to the reduced motion of water [23]. It is suggested that decreased ADC value is associated with increased stromal collagen and vascular endothelial growth factor (VEGF), which plays an important role in the neovasculature formation in tumor stroma [28]. Ma et al. also observed significant negative correlations of ADC with the VEGF expression and grade in prostate cancer [29]. Huang et al. also found a negative correlation between VEGF expression and the ADC values of hepatocellular carcinoma [30]. In another study, it was demonstrated that the diffusion of water molecules is also restricted by extracellular components, such as collagen fibers and extracellular matrix [31]. On the other hand, overexpressed VEGF, which is linked to increased

permeability of thecal blood vessels, angiogenesis, and connective tissue stroma generation in the ovarian stroma of PCOS, has been reported [32]. Moreover, Papachroni et al. revealed that increased distribution of collagen type IV in the polycystic ovary tissue induces cystogenesis [33]. The main principle of the monoexponential model of DWI is the quantification of Brownian motion which reflects the diffusion motion of water molecules in tissues [34]. In this model, obtained ADC information reflects both diffusion motion of water molecules and capillary perfusion of the microcirculatory network [10, 34–36]. This limitation could be overcome by the IVIM MRI, which separates molecular diffusion and microcirculatory perfusion-related diffusion, assessing the motion of the water in non-exchanging intravascular and extravascular compartments [10]. In IVIM MRI, both D^* and f reflect the perfusion in the capillary network and the blood volume in the tissue. A diminished D^* or f value is meaningful for diminished capillary perfusion and blood volume [11, 37]. In our study, we revealed higher D^* , f with reduced ADC values in patients with PCOS than healthy controls. However, we found no significant difference between patient and control groups in comparison with D_{true} . Although we did not assess the cellular mechanism of PCOS, we suggest that decreased ADC values with increased IVIM MRI-derived perfusion parameters (D^* and f values) would be explained increased extracellular matrix, angiogenesis, and vascularization. This was also mentioned in various Doppler ultrasound studies performed on PCOS patients [38–40]. Battaglia et al. showed increased vascularization and high pulsatility index with a typical decreased resistive index in the ovarian stroma [39]. Lam et al. also demonstrated lower resistive index and pulsatility index in two-dimensional Doppler and higher vascularization flow index and vascularization index in three-dimensional power Doppler in patients with PCOS [40]. Our study is the only study that assessed IVIM MRI-derived parameters in

patients with PCOS. Moreover, Panchal et al. [41] suggested that elevated LH level increases stromal vascularization by stimulating neoangiogenesis in patients with PCOS. Increased ovarian fibrosis was demonstrated in androgen-induced PCOS rats [42]. Cıracı et al. [43] also showed the increased stromal stiffness by real-time ultrasound elastography in patients with PCOS. In this study, they found an increased strain ratio which showed moderate positive correlations with ovarian volume and follicle count. However, we found no significant difference in terms of D_{true} between the two groups. In liver fibrosis, decreased D_{true} value with perfusion parameters (D^* and f values) was found compared to the healthy liver, which is negatively correlated with the severity of hepatic fibrosis [44, 45]. However, they found no significant difference in terms of D_{true} in further studies [20, 46]. The result of our study may be caused by the variation of the disease, such as the peripheral or general cystic patterns of PCOS and different ages of fibrosis. Differences in treatment, complex and multifactorial pathogenesis (polycystic ovarian morphology, hyperandrogenemia, insulin resistance, obesity, etc.) suggest the multifactorial nature, including genetic, environmental components, and heterogeneity of the syndrome [47].

The main advantages of the technique are to be non-invasive, are not requiring contrast agents and ionizing radiation, and provide quantitative information, fast and easy to performance into routine practice. In recent years, ovarian morphology has been increasingly evaluated by MRI in several studies [7, 9, 48]. MRI has an advantage for imaging ovaries with high-contrast resolution in adolescents and obese women. Although perfusion MRI was not studied in patients with PCOS, it is mentioned that DWI and MRI perfusion have approximately the same sensitivity and positive impact on operative management [49]. Further studies comparing IVIM MRI-derived perfusion and diffusion parameters with either histopathological findings of perfusion MRI will be useful for elucidating the hypothesis underlying the pathogenesis. Additionally, compared IVIM MRI studies that assess the response to the therapy are required.

Our study has some limitations, including a small sample size and a lack of correlation between IVIM MRI-derived parameters and the factors that play a role in the PCOS mechanism. And also, we did not assess the IVIM MRI-derived parameters of the ovarian stroma in PCOS patients in response to the various treatments. Moreover, the IVIM DWI has its own limitations. Scanner and field intensities, physiological activities of the tissue [50], and motion artifacts may affect the result. Lack of consensus on the number and distribution of b values is the other limitation of the DWI and IVIM MRI techniques. To overcome these limitations, the measurement

was revealed from the mean of four ROI values for each observer. Further research correlated with the factors that play a role in the mechanism of PCOS in a larger cohort is required.

Conclusions

In conclusions, our study results showed that values of IVIM-derived parameters of the ovarian stroma are higher in patients with PCOS than in control subjects. IVIM MRI may be a useful imaging tool in diagnosis of PCOS with a good-to-excellent agreement and with an acceptable sensitivity and specificity. It can be revealed routinely and safely without radiation exposure and using a contrast agent. IVIM MRI would be added to image ovaries especially in overweighted and virgin patients.

Abbreviations

MRI: Magnetic resonance imaging; IVIM: Intravoxel incoherent motion; PCOS: Polycystic ovary syndrome; LH: Luteinizing hormone; FSH: Follicle-stimulating hormone; DHEA: Dehydroepiandrosterone and dehydroepiandrosterone sulfate; TSH: Thyroid-stimulating hormone; D : True diffusion or slow diffusion coefficient; D^* : Pseudo-diffusion or fast diffusion coefficient; f : Perfusion fraction; ADC: Apparent diffusion coefficient; ICC: Interclass correlation coefficient; ROC: Receiver operating characteristic.

Acknowledgements

Not applicable.

Author contributions

SO interpreted all images and wrote discussion section. MBD, MH, MS and BC collected data and wrote introduction as well as Material and Method. AA managed this project and edited manuscript. We confirm that all of us as we are the authors accept the manuscript for submission. All authors read and approved the final manuscript.

Funding

There was no source of funding.

Availability of data and materials

The datasets used and/or analyzed during the current study are available from the corresponding author on reasonable request.

Declarations

Ethics approval and consent to participate

This study has been ethically approved by the ethics committee of Istanbul Medeniyet University (ID Number, 2019/0156). Written informed agreement was obtained from all the cases.

Consent for publication

Written consent to publish this information was obtained from study participants, and proof of consent to publish from study participants can be requested at any time.

Competing interests

The authors have no potential conflicts of interest to disclose.

Author details

¹Department of Radiology, Goztepe Training and Research Hospital, Istanbul Medeniyet University, Istanbul, Turkey. ²Department of Endocrinology, Goztepe Training and Research Hospital, Istanbul Medeniyet University, Istanbul, Turkey. ³Department of Obstetrics and Gynecology, Goztepe Training and Research Hospital, Istanbul Medeniyet University, Istanbul, Turkey.

Received: 28 April 2022 Accepted: 30 September 2022
Published online: 07 October 2022

References

- Rosenfield RL, Ehrmann DA (2016) The Pathogenesis of Polycystic Ovary Syndrome (PCOS): the hypothesis of PCOS as functional ovarian hyperandrogenism. *Revisit Endocr Rev* 37:467–520
- Dumesic DA, Oberfield SE, Stener-Victorin E et al (2015) Scientific statement on the diagnostic criteria, epidemiology, pathophysiology, and molecular genetics of polycystic ovary syndrome. *Endocr Rev* 36:487–525
- Rotterdam ESHRE/ASRM-Sponsored PCOS Consensus Workshop Group Revised (2003) Consensus on diagnostic criteria and long-term health risks related to polycystic ovary syndrome. *Fertil Steril* 2004(81):19–25
- Dewailly D, Lujan ME, Carmina E et al (2014) Definition and significance of polycystic ovarian morphology: a task force report from the Androgen Excess and Polycystic Ovary Syndrome. *Soc Hum Reprod Update* 20:334–352
- Barber TM, McCarthy MI, Wass JA et al (2006) Obesity and polycystic ovary syndrome. *Clin Endocrinol (Oxf)* 65:137–145
- Barber TM, Alvey C, Greenslade T et al (2010) Patterns of ovarian morphology in polycystic ovary syndrome: a study utilising magnetic resonance imaging. *Eur Radiol* 20:1207–1213
- Nylander M, Frøssing S, Bjerre AH et al (2017) Ovarian morphology in polycystic ovary syndrome: estimates from 2D and 3D ultrasound and magnetic resonance imaging and their correlation to anti-Müllerian hormone. *Acta Radiol* 58:997–1004
- Yoo RY, Sirlin CB, Gottschalk M et al (2005) Ovarian imaging by magnetic resonance in obese adolescent girls with polycystic ovary syndrome: a pilot study. *Fertil Steril* 84:985–995
- Le Bihan D, Breton E, Lallemand D et al (1988) Separation of diffusion and perfusion in intravoxel incoherent motion MR imaging. *Radiology* 168:497–505
- Koh DM, Collins DJ, Orton MR (2011) Intravoxel incoherent motion in body diffusion-weighted MRI: reality and challenges. *AJR Am J Roentgenol* 196:1351–1361
- Le Bihan D, Breton E, Lallemand D et al (1986) MR imaging of intravoxel incoherent motions: application to diffusion and perfusion in neurologic disorders. *Radiology* 161:401–407
- Le Bihan D, Turner R (1992) The capillary network: a link between IVIM and classical perfusion. *Magn Reson Med* 27:171–178
- Le Bihan D, Turner R, Moonen CT et al (1991) Imaging of diffusion and microcirculation with gradient sensitization: design, strategy, and significance. *J Magn Reson Imaging* 1:7–28
- Tao YY, Zhou Y, Wang R et al (2020) Progress of intravoxel incoherent motion diffusion-weighted imaging in liver diseases. *World J Clin Cases* 8:3164–3176
- Manoharan D, Das CJ, Aggarwal A et al (2016) Diffusion weighted imaging in gynecological malignancies—present and future. *World J Radiol* 8:288–297
- Mannelli L, Nougaret S, Vargas HA et al (2015) Advances in diffusion-weighted imaging. *Radiol Clin N Am* 53:569–581
- Dixon WT (1988) Separation of diffusion and perfusion in intravoxel incoherent motion MR imaging: a modest proposal with tremendous potential. *Radiology* 168:566–567
- Le Bihan D (1988) Intravoxel incoherent motion imaging using steady-state free precession. *Magn Reson Med* 7:346–351
- Luciani A, Vignaud A, Cavet M et al (2008) Liver cirrhosis: intravoxel incoherent motion MR imaging-pilot study. *Radiology* 249:891–899
- Lautt WW (1977) Hepatic vasculature: a conceptual review. *Gastroenterology* 73:1163–1169
- Landis JR, Koch GG (1977) The measurement of observer agreement for categorical data. *Biometrics* 33:159–174
- Padhani AR, Liu G, Koh DM et al (2009) Diffusion-weighted magnetic resonance imaging as a cancer biomarker: consensus and recommendations. *Neoplasia* 11:102–125
- He M, Song Y, Li H et al (2020) Histogram analysis comparison of monoexponential, advanced diffusion-weighted imaging, and dynamic contrast-enhanced MRI for differentiating borderline from malignant epithelial ovarian tumors. *J Magn Reson Imaging* 52:257–268
- Xiao Z, Tang Z, Zhang J et al (2020) Whole-tumor histogram analysis of monoexponential and advanced diffusion-weighted imaging for sinonasal malignant tumors: correlations with histopathologic features. *J Magn Reson Imaging* 51:273–285
- Ding Y, Tan Q, Mao W et al (2019) Differentiating between malignant and benign renal tumors: Do IVIM and diffusion kurtosis imaging perform better than DWI? *Eur Radiol* 29:6930–6939
- Deveer M, Deveer R, Cullu N et al. The added value of diffusion-weighted MRI in diagnosis of polycystic ovary syndrome: a preliminary study. *Eur Congr Radiol ECR*. <https://doi.org/10.1594/ecr2016/B-1326>
- Samanci C, Alis D, Ustabasioglu FE et al (2017) Apparent diffusion coefficient measurement of ovarian stroma: a potential tool for the diagnosis of polycystic ovary syndrome. *Diagn Interv Imaging* 98:57–61
- Aoyagi T, Shuto K, Okazumi S et al (2012) Apparent diffusion coefficient correlation with oesophageal tumour stroma and angiogenesis. *Eur Radiol* 22:1172–1177
- Ma T, Yang S, Jing H et al (2018) Apparent diffusion coefficients in prostate cancer: correlation with molecular markers Ki-67, HIF-1 α and VEGF. *NMR Biomed*. <https://doi.org/10.1002/nbm.3884>
- Huang Z, Meng X, Xiu J et al (2014) MR imaging in hepatocellular carcinoma: correlations between MRI features and molecular marker VEGF. *Med Oncol* 31:313
- Hauge A, Wegner CS, Gaustad JV et al (2017) Diffusion-weighted MRI-derived ADC values reflect collagen I content in PDX models of uterine cervical cancer. *Oncotarget* 8:105682–105691
- Kamat BR, Brown LF, Manseau EJ et al (1995) Expression of vascular permeability factor/vascular endothelial growth factor by human granulosa and theca lutein cells. Role in corpus luteum development. *Am J Pathol* 146:157–165
- Papachroni KK, Piperi C, Levidou G et al (2010) Lysyl oxidase interacts with AGE signalling to modulate collagen synthesis in polycystic ovarian tissue. *J Cell Mol Med* 14:2460–2469
- Taouli B, Koh DM (2010) Diffusion-weighted MR imaging of the liver. *Radiology* 254:47–66
- Bammer R (2003) Basic principles of diffusion-weighted imaging. *Eur J Radiol* 45:169–184
- Lewis S, Dyvorne H, Cui Y et al (2014) Diffusion-weighted imaging of the liver: techniques and applications. *Magn Reson Imaging Clin N Am* 22:373–395
- Wolff D, van Melle JP, Dijkstra H et al (2016) The Fontan circulation and the liver: a magnetic resonance diffusion-weighted imaging study. *Int J Cardiol* 1(202):595–600
- Bozkurt M, Kara Bozkurt D, Kurban D et al (2021) 2-D and 3-D ultrasonographic characteristics of the ovary in women with PCOS and multifollicular ovaries. *J Obstet Gynaecol* 41:920–926
- Battaglia C, Artini PG, D'Ambrogio G et al (1995) The role of color Doppler imaging in the diagnosis of polycystic ovary syndrome. *Am J Obstet Gynecol* 172:108–113
- Lam PM, Johnson IR, Raine-Fenning NJ (2007) Three-dimensional ultrasound features of the polycystic ovary and the effect of different phenotypic expressions on these parameters. *Hum Reprod* 22:3116–3123
- Panchal S, Nagori CB (2012) Baseline scan and ultrasound diagnosis of PCOS. *Donald School J Ultrasound Obst Gynecol* 6:290–299
- Wang D, Wang W, Liang Q et al (2018) DHEA-induced ovarian hyperfibrosis is mediated by TGF- β signaling pathway. *J Ovarian Res* 10(11):6
- Ciraci S, Tan S, Özcan AS et al (2015) Contribution of real-time elastography in diagnosis of polycystic ovary syndrome. *Diagn Interv Radiol* 21:118–122
- Chen C, Wang B, Shi D et al (2014) Initial study of biexponential model of intravoxel incoherent motion magnetic resonance imaging in evaluation of the liver fibrosis. *Chin Med J* 127:3082–3087
- Hu G, Chan Q, Quan X et al (2015) Intravoxel incoherent motion MRI evaluation for the staging of liver fibrosis in a rat model. *J Magn Reson Imaging* 42:331–339
- Wu CH, Ho MC, Jeng YM et al (2015) Assessing hepatic fibrosis: comparing the intravoxel incoherent motion in MRI with acoustic radiation force impulse imaging in US. *Eur Radiol* 25:3552–3559

47. Hoeger KM, Dokras A, Piltonen T (2021) Update on PCOS: consequences, challenges, and guiding treatment. *J Clin Endocrinol Metab* 8(106):e1071–e1083
48. Brown M, Park AS, Shayya RF et al (2013) Ovarian imaging by magnetic resonance in adolescent girls with polycystic ovary syndrome and age-matched controls. *J Magn Reson Imaging* 38:689–693
49. El Ameen NF, Eissawy MG, Mohsen LAMS et al (2020) MR diffusion versus MR perfusion in patients with ovarian tumors: How far could we get? *Egypt J Radiol Nucl Med* 51:35
50. Neil JJ, Bretthorst GL (1993) On the use of Bayesian probability theory for analysis of exponential decay data: an example taken from intravoxel incoherent motion experiments. *Magn Reson Med* 29:642–647

Publisher's Note

Springer Nature remains neutral with regard to jurisdictional claims in published maps and institutional affiliations.

Submit your manuscript to a SpringerOpen[®] journal and benefit from:

- ▶ Convenient online submission
- ▶ Rigorous peer review
- ▶ Open access: articles freely available online
- ▶ High visibility within the field
- ▶ Retaining the copyright to your article

Submit your next manuscript at ▶ [springeropen.com](https://www.springeropen.com)
